INTER-INDIVIDUAL ORGAN-DRIVEN CT REGISTRATION FOR DOSE MAPPING IN PROSTATE CANCER RADIOTHERAPY

Gaël Dréan[1,2], *Oscar Acosta*[1,2], *Antoine Simon*[1,2], *Renaud de Crevoisier*[1,2,3] *and Pascal Haigron*[1,2]

[1] INSERM, U642, Rennes, F-35000, France;
[2] Université de Rennes 1, LTSI, Rennes, F-35000, France;
[3]Département de Radiothérapie, Centre Eugène Marquis, Rennes, F-35000, France

ABSTRACT

Toxicity prediction is crucial in prostate cancer radiotherapy. There is thus a need to model voxel-wise relationships between dose distribution and toxicity events. However, building such a model is challenging due to difficulties in the mapping of the organs and of the dose distribution. We designed an organ-driven registration method merging the deformation fields computed for registrations first of the computed tomography scans and second of the organs delineations. The merging was done by weighting the different deformation fields according to the distance between voxels and organs. We evaluated this strategy on 29 individuals and compared the results with those obtained with intensity-based affine and non-rigid registrations. The dice scores obtained were above 0.9 for each organ ans the accuracy was improved by 41.1% for the prostate, 31.5% for the bladder and 54.2% for the rectum. The method allows to accurately map inter-individual dose distributions to a single coordinate system to perform further voxel-based statistical analysis.

***Index Terms*—** Image Registration, Organs Matching, Prostate Cancer Radiotherapy

1. INTRODUCTION

Predictive models of toxicity in prostate cancer radiotherapy are traditionally based on dose-volume Histograms (DVH). Nevertheless, these models lack of spatial accuracy since they waste the rich spatial information of the dose by reducing the dimensionality to a 1D function. In order to unravel the subtle dose-effect relationships across a population, 3D images should be thoroughly analyzed at a voxel level taking into account the spatial distribution. Inter-individual voxel-wise comparisons are only allowed if anatomical and dosimetric data are represented in the same common coordinate system [1]. Accurate inter-individual registration is thus a required previous step in this process where a simultaneous matching of prostate and organs at risk (rectum, bladder) will allow to map the dose distributions and then to perform accurate studies of toxicity and failure as in [2, 3]. Recent studies use voxel-wise analysis of the dose distributions to predict toxicity in the urinary tract [4] and tumor control in prostate [5]. However, these methods are approximative in terms of spatial location as the mapping is defined by a parametric representation of the whole image with respect to the organs position in polar coordinates.

Registering CTs is particularly challenging because of the poor soft-tissue contrast, the large inter-individual variability and the filling differences of the bladder and the rectum [6]. In this context, it has been shown that a pure intensity based registration is not accurate as required and may lead to local errors [7]. Hence, all the complementary knowledge about the individuals' anatomy should be used to improve the performance of the registration. Some solutions have been proposed to use organs information to register CT to CBCT in an intra-individual context. In 2009, Greene [8] introduced a Constrained Non-Rigid Registration based on the Free-Form Deformation (FFD) algorithm [9]. After a rigid registration step, they registered the binary planning-day and treatment-day organ delineations. Then, they used these computed transformations to constrain the global deformation. This work showed that more accurate registration results can be obtained by adding constraints on the control points. Lu [10] proposed first a hard-constrained non-rigid registration using Lagrange multipliers method [11] and then introduced a bayesian framework, which assumed prior models. This probabilistic formulation improved the registration accuracy. Other authors [12, 13] used organ delineations to introduce relationships between the voxels inside the organs to constrain the non-rigid registration [15]. However, those methods still remain to be explored in an inter-individual context where the anatomical differences are greater and larger deformations may be needed.

In this paper we present a new organ-driven non-rigid registration method devised to provide an accurate matching between organs for inter-individual mapping of dose. Unlike [8, 10, 11], our model is based on the diffeomorphic demons algorithm [15] exhibiting three interesting properties in the context of voxel-wise statistical analysis: (i) accurate matching of CT-Scan information (skin and bony structures) and organs (both, the barycenters and the boundaries), (ii) speed and easy parametrization and (iii) contours sensitivity. We introduce here an hybrid method that takes advantage of information available during the planning process, namely the CT and the organs delineations whose distance maps (DM) are normalized and computed, allowing simultaneous organ-wise registration. First, a CT-to-CT registration provides accurate alignment for the skin and the bones. Then registrations between normalized DM for each organ drive the whole deformation. Our method combines the different computed Deformation Fields, by weighting them according to the distance to the considered organs. We compared our method with intensity-based registration algorithms, namely Affine *Block-Matching* [16], non-rigid Free-Form Deformation (FFD) [9, 17], and non-rigid diffeomorphic demons [15].

2. MATERIALS & METHODS

2.1. Data

We carried out a study on 30 prostate cancer patients, treated with external radiotherapy. Each individual underwent a planning CT. All acquired CT were 2mm thickness slice with a 512×512 1mm pixels resolution in the axial plan.

For each individual, the organs were manually delineated by the same expert, following the standard clinical protocol in radiotherapy. The expert contoured the clinical targets - namely the prostate and the seminal vesicles - and the organs at risk (OAR): the bladder and the rectum. In this study, only the CT and the delineated prostate, bladder and rectum were considered (Fig.1).

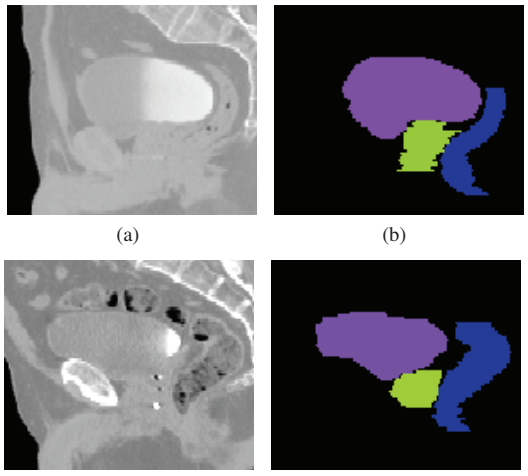

Fig. 1. Example of two CT sagittal views ((a) individual and (c) template) with the delineated organs ((b) and (d)): prostate (green), bladder (mauve) and rectum (blue)

2.2. Description of the Algorithm

The overall idea of our *Deformation Fields Merging* method (DFM) is presented in figure 2. First, one individual among the 30 has been randomly selected as a template. We followed 4 main steps: first, a pre-processing step in which the DMs from the organs delineations were computed, second, an initialization step where an affine followed by a non-liner demons registration were performed between CT-scans, and between inter-individual normalized DMs, and eventually the merging step where the different computed deformations fields ($\overrightarrow{DF}$) were weighted and combined according to the distances to the different organs.

2.2.1. *Image Pre-Processing: Distance Maps Computations*

DMs were computed for each individual's organs, namely the prostate, the bladder and the rectum. That step consisted in computing the euclidean distance map from the organ manual delineation with the following convention: the distance in mm is positive inside the organ and negative outside (Fig 3 - (a) and (d)).
For each couple Template/individual, 6 normalized DMs were computed: 3 for the individual itself, and 3 for the template, corresponding to the 3 considered organs. The region inside each organ was normalized with respect to the corresponding template's organ by multiplying the distance by the maximum inside the organs template. The same procedure was applied to the template DMs. Then, these 6 DMs, were masked by these new normalized organ-restricted DMs (Fig 3 - (b) and (e)). This normalization was aimed at aligning the boundaries and the barycenters of the structures with respect to the template.
In the following, these notations were used:

- $DM^{i}_{\omega\in\Omega}$: Distance Map of an organ $\omega \in \Omega = \{$Prostate, Bladder, Rectum $\}$ of the individual $i \in \{$ Template, Individuals $\}$
- $\hat{DM}^{i,j}_{\omega\in\Omega}$: Normalized organ-restricted of an organ $\omega \in \Omega$ of an the individual i by the maximum of the DM^{j}_{ω}

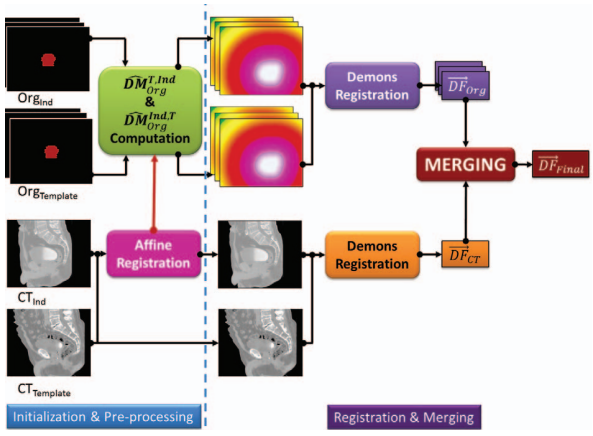

Fig. 2. Pipeline of the registration algorithm.

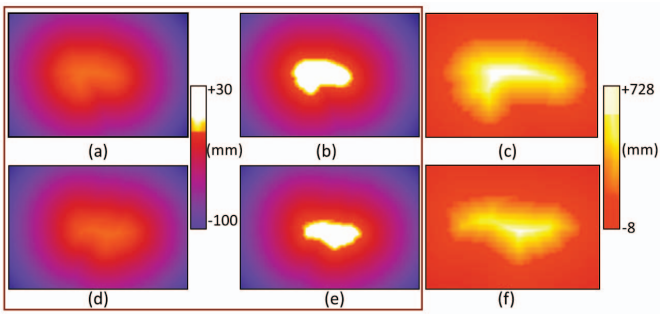

Fig. 3. Example of DMs for (a) an individual's bladder and for (d) the template (T); Exemple of normalized DM for (b-c) the individual and (e-f) the template.

2.2.2. *Initialization: Affine Registration*

We used the *Block-Matching* algorithm introduced by Ourselin [16] using the Normalized Mutual Information as similarity measure to register the CT images. Once computed, the affine transformation has been applied to the delineated organs and to the different $\hat{DM}^{i,j}_{\Omega}$ to propagate them into the common space.

2.2.3. *Non-Rigid Registration*

We used the diffeomorphic demons algorithm introduced by Vercauteren [15] to register first the individual's CT to the Template's CT and then the i-individual $\hat{DM}^{Ind_i,T}_{\omega\in\Omega}$ to the $\hat{DM}^{T,Ind_i}_{\omega\in\Omega}$ for each considered organ (prostate, bladder and rectum). At the end of this step we had 4 different $\overrightarrow{DF}$.

2.2.4. *Deformation Fields Merging*

The merging of the 4 $\overrightarrow{DF}$ (CT, prostate, bladder and rectum) was based on the following assumption: the closer a voxel is from an organ, the stronger its link to this organ. Then, the four previously computed $\overrightarrow{DF}$ were merged by weighting them according to the distance between voxels and the organs.

Our algorithm took 10 inputs, namely:

- $DM^{Template}_{\omega\in\Omega}$
- $\overrightarrow{DF}_{\mathbf{k}\in\mathbf{K}}$: the $\overrightarrow{DF}$ of one element of $K = \{\ CT, \hat{DM}^{T,Ind_i}_{\omega\in\Omega}\ \}$
- $O^{T\cup Ind_i}_{\omega\in\Omega}$: the image of the union of the individual's affine-registered and the template $\Omega = \{$Prostate,Bladder,Rectum$\}$ dilated of 2 voxels.

Then, when the images were went through, two cases were possible: either the voxel is in at least one of the three $O_{\omega\in\Omega}^{T\cup Ind_i}$ (case 1) or not (case 2). Then, the final merged $\overrightarrow{DF}$ on the voxel x ($\overrightarrow{DF}_{Final}(x)$) was computed:

- if case 1: $\overrightarrow{DF}_{\mathbf{Final}}(x)$ is computed with the equation (1):

$$\overrightarrow{DF}_{\mathbf{Final}}(x) = \sum_{\omega_1\in\Omega_1} \frac{1_{\{x\in\omega_1\}}}{\sum_{\omega_2\in\Omega_2} 1_{\{x\in\omega_2\}}} \overrightarrow{DF}_{\omega_1\in\mathbf{\Omega_1}}(x), \quad (1)$$

where $\Omega_1 = \Omega_2 = \{$ Prostate, Bladder, Rectum $\}$, and $1_{\{\cdot\in\omega\}}$ the indicator function of ω.

- if case 2: $\overrightarrow{DF}_{\mathbf{Final}}(x)$ is computed with the equation (2):

$$\overrightarrow{DF}_{\mathbf{Final}}(x) = \frac{1}{\Delta}\left[\delta_{CT}\overrightarrow{DF}_{\mathbf{CT}}(x) + \sum_{\omega\in\Omega}\delta_{\omega\in\Omega}\overrightarrow{DF}_{\omega\in\mathbf{\Omega}}(x)\right], \quad (2)$$

with:

- $d_{x,\omega}$ is the Euclidean distance between the voxel x and the organ $\omega\in\Omega$
- $\delta_{CT} = 1 - \exp\left(-\sum_{\omega} d_{x,\omega}^2\right)$
- $\delta_{\omega} = \exp\left(-d_{x,\omega}^2\right)$
- $\Delta = \delta_{CT} + \sum_{\omega}\delta_{\omega}$

3. EXPERIMENTS

Experiments were carried out to firstly evaluate the registration between the normalized distance maps only ($\hat{DM}_{\omega\in\Omega}^{Ind_i,T}$ and $\hat{DM}_{\omega\in\Omega}^{T,Ind_i}$), and secondly to compare the performance of our organ-driven *Deformation Fields Merging* strategy with intensity-based registration methods. Thus, 29 individuals were registered to the randomly-selected template using Affine registration [16], Affine + non-rigid Free-Form Deformation registration (FFD) [9, 17], and Affine + demons registration, and our *Deformation Fields Merging* strategy. Finally, we propagated the 29 individuals' organs and dose distribution to the common space (template).
The accuracy of the registration methods was first assessed by computing the coincidence between the individuals' registered organs and the organs of the template. We used the *dice score*, defined as $Dice = 2|A\cap B|/|A| + |B|$, where $|\cdot|$ indicates the number of voxels of the considered A and B volumes. We computed also the euclidean distance between the barycenters of each individual's organ and the counterpart in the template after registration.

4. RESULTS

The intermediate non-rigid registration between only the normalized DMs of the organs allows to achieve accurate results, as shows the average dice score of 0.95 ± 0.01 for the prostate, 0.98 ± 0.01 for the bladder, 0.93 ± 0.02 for the rectum. The computed average distance (mm) between the barycenters was 0.69 ± 0.5 for the prostate, 0.1 ± 0.3 for the bladder and 1.1 ± 0.7.
Then, we carried out an exploratory analysis of dice scores obtained with the different registration strategies. Figure (5) shows the results by comparing the Dices Score for each organ and each methods. These results shows that our new DFM strategy provides significantly more accurate results than Demons (t-test,$p < 0.001$), with an average dice score of 0.92 ± 0.026 for the prostate, 0.98 ± 0.01 for the bladder, 0.92 ± 0.03 for the rectum, with, in addition, lower variances. Furthermore, these observations are confirmed for the barycenters alignment, as shown in Tab. 1.
Figure 4 shows a representative example of the obtained registration between an individual (Fig. 4(a)) and the template (Fig. 4(b)): Figure 4(c) shows the final deformation field and Figure 4(d) illustrates, with a checkerboard view, the coincidence between the CT of the individual and of the template.

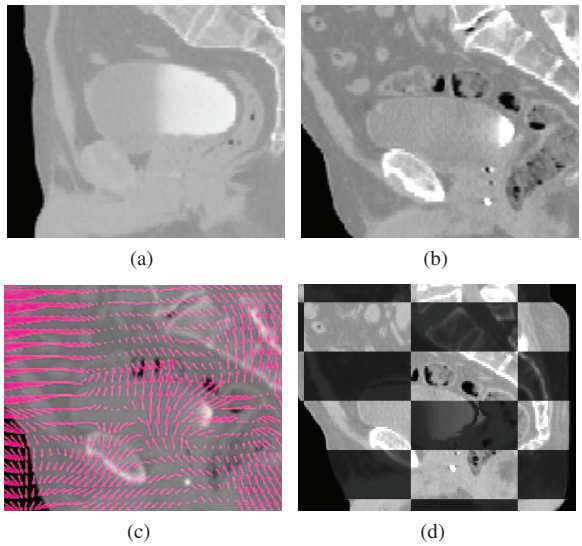

Fig. 4. Example of registration between (a) an individual and (b) the template: (c) computed merged Deformation Field and (d) CheckerBoard view between the CT of the template (light gray) and the registered CT of an individual (dark gray)

	Affine	FFD	Demons	DFM
Prostate	11.1 ± 5.1	8.3 ± 4.6	7.1 ± 4.2	1.1 ± 0.7
Bladder	16.1 ± 5.9	12.2 ± 6.0	8.2 ± 5.2	0.4 ± 0.7
Rectum	13.1 ± 5.4	11.8 ± 5.9	12.3 ± 5.4	1.2 ± 0.8

Table 1. Mean Euclidean distance (mm) between the barycenter of the registered organs and of the template organs for each registration method.

5. CONCLUSION AND DISCUSSION

In this paper we proposed an original organ-driven non-rigid registration strategy for dose mapping in prostate cancer radiotherapy. We first evaluated the results of the registration between normalized organs distance map. These results suggest that each single organ can be independently well registered. This registration method allows then to achieve a good tradeoff between the registration of the CTs and of all the organs. Indeed, exploiting the individuals' planning data and based on a weighted merging of the Deformation Fields, our new *Deformation Fields Merging* strategy provides more accurate results than gray-levels intensity based non-rigid registration algorithms, as shown in figure 5.

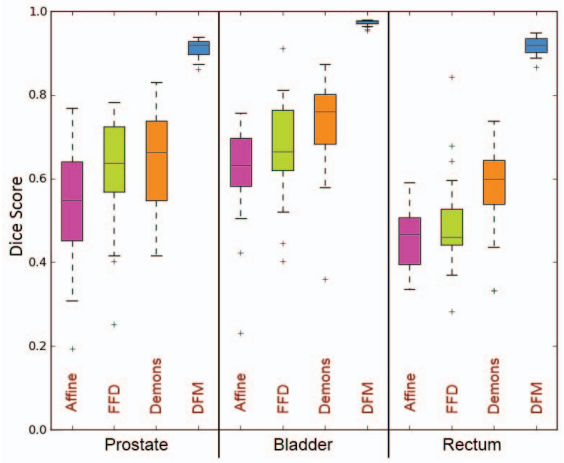

Fig. 5. Experimental results: dice scores comparison for each organ.

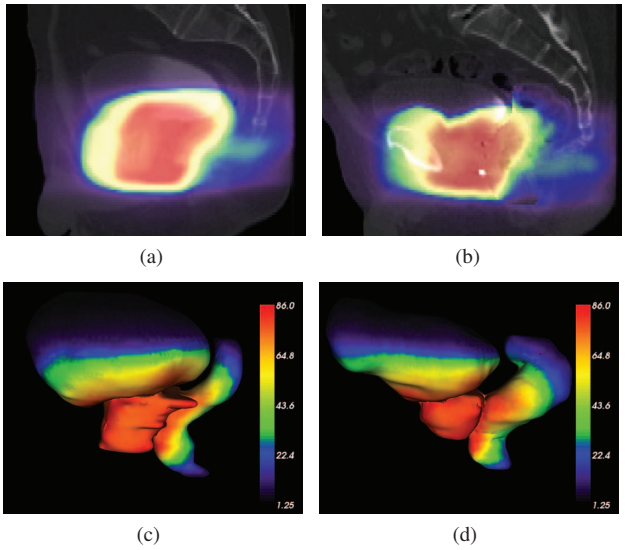

(a) (b) (c) (d)

Fig. 6. Individual's dose distribution computed during the radiotherapy planning overlaid on a) the individual's the CT in the native space ; b) propagated, using a trilinear interpolation, towards the template coordinate system. c) 3D representation of prostate, bladder and rectum with the corresponding dose distribution in the individual's space and d) propagated to the template 3D structures.

The present work opens the way to accurate voxel-based comparison across a population aimed at building predictive models of toxicity and failure. Indeed, these registration transformations can be applied to the individuals dose distributions, using a trilinear interpolation, as shown in Fig. 6. Accurate registration results are then crucial to perform a voxel-wise statistical analysis of the individuals' dose distributions, to analyze the contribution of each voxel to the occurrence of toxicity events and thus to identify the heterogeneous intra-organs radio-sensitivity. Future work includes the development of an iterative similar strategy, minimizing a cost function based on the similarity between the distance maps, and allowing the merging of the different deformation fields at each iteration.

6. REFERENCES

[1] O. Acosta, *et al.*, "Atlas based segmentation and mapping of organs at risk from planning ct for the development of voxel-wise predictive models of toxicity in prostate radiotherapy", in *MICCAI'10*, 2010, vol. 6367 of *LNCS*, pp. 42–51.

[2] Chen B., *et al.*, "Spatial Characterization and Classification of Rectal Bleeding in Prostate Cancer Radiotherapy with a Voxel-Based Principal Components Analysis Model for 3D Dose Distribution", in *MICCAI'11*, 2011, vol. 6963 of *LNCS*, pp. 60–69.

[3] Ospina J. *et al.*, "Spatial Nonparametric Mixed-Effects Models with Spatial-Varying Coefficients for Analysis of Populations", in *MLMI MICCAI'11*, 2011, vol. 2011 of *LNCS*, pp. 142–150.

[4] W. D. Heemsbergen, *et al.*, "Urinary obstruction in prostate cancer patients from the dutch trial (68 Gy vs. 78 Gy): Relationships with local dose, acute effects, and baseline characteristics," *Int. Jour. of Rad. Onc.*, vol. 78, no. 1, pp. 19 – 25, 2010.

[5] M. G. Witte, *et al.*, "Relating dose outside the prostate with freedom from failure in the dutch trial 68 gy vs. 78 gy," *Int. Journ. of Rad. Onc.*, vol. 77, no. 1, pp. 131 – 138, 2010.

[6] O. Acosta, *et al.*, "Evaluation of multi-atlas-based segmentation of ct scans in prostate cancer radiotherapy," in *IEEE ISBI*, 2011, pp. 1966 –1969.

[7] G. Dréan, *et al.*, "Evaluation of inter-individual pelvic CT-scans registration," *IRBM.*, vol. 32, no. 5, pp. 288 – 292, 2011.

[8] W.H. Greene, *et al.*, "Constrained non-rigid registration for use in image-guided adaptive radiotherapy," *MedIA*, vol. 13, no. 5, pp. 809–817, 2009.

[9] D. Rueckert, *et al.*, "Nonrigid registration using free-form deformations: Application to breast MR images," *IEEE TMI*, vol. 18, pp. 712–721, 1999.

[10] C. Lu, *et al.*, "Constrained non-rigid registration using lagrange multipliers for application in prostate radiotherapy," in *CVPRW IEEE*, 2010, pp. 133–138.

[11] C. Lu, *et al.*, "An integrated approach to segmentation and nonrigid registration for application in image-guided pelvic radiotherapy.," *MedIA*, 2011.

[12] T. Chen, *et al.*, "Object-constrained meshless deformable algorithm for high speed 3D nonrigid registration between CT and CBCT," *MedIA*, vol. 37, pp. 197, 2010.

[13] G. Cazoulat, *et al.*, "Dose monitoring in prostate cancer radiotherapy using cbct to ct constrained elastic image registration," *PCI MICCAI'11*, vol. 6963 of LNCS pp. 70–79, 2011.

[14] J.-P. Thirion, "Image matching as a diffusion process: an analogy with Maxwell's demons," *MedIA*, vol. 2, no. 3, pp. 243 – 260, 1998.

[15] T. Vercauteren, *et al.*, "Non-parametric Diffeomorphic Image Registration with the Demons Algorithm," in *MICCAI'07*, 2007, vol. 4792/2007 of *LNCS*, pp. 319–326.

[16] S. Ourselin, *et al.*, "Reconstructing a 3D structure from serial histological sections," *Image and Vision Computing*, vol. 19, no. 1-2, pp. 25 – 31, 2001.

[17] M. Modat, *et al.*, "Fast free-form deformation using graphics processing units," *Computer Methods and Programs in Biomedicine*, vol. 98, no. 3, pp. 278 – 284, 2010,